

Impact parameter dependence of J/ψ and Drell-Yan production in heavy ion collisions at $\sqrt{s_{NN}}=17.3$ GeV

V. Emel'yanov,¹ A. Khodinov,¹ S. R. Klein,² and R. Vogt^{2,3}

¹*Moscow State Engineering Physics Institute (Technical University), Kashirskoe ave. 31, Moscow 115409, Russia*

²*Nuclear Science Division, Lawrence Berkeley National Laboratory, Berkeley, California 94720*

³*Physics Department, University of California, Davis, California 95616*

(Received 31 August 1998)

In heavy-ion collisions, J/ψ and Drell-Yan production are expected to be affected by nuclear modifications to the free nucleon structure functions. If these modifications, referred to here as shadowing, are proportional to the local nuclear density, the per nucleon cross sections will depend on centrality. Differences in quark and gluon shadowing will lead to a new source of impact parameter dependence of the J/ψ to Drell-Yan production ratio. We calculate this ratio in the CERN NA50 acceptance with several shadowing parametrizations to explore its centrality dependence. [S0556-2813(99)50704-8]

PACS number(s): 25.75.Dw, 21.65.+f, 24.85.+p

A significant ‘‘anomalous’’ suppression of J/ψ production has been observed in Pb+Pb collisions. The ratio of J/ψ to Drell-Yan production is lower in central Pb+Pb collisions than extrapolations from more peripheral collisions, lighter ion interactions, and pA collisions suggest [1]. Centrality is inferred from the transverse energy, E_T .

Almost all calculations of J/ψ and Drell-Yan production in nuclear collisions to date have been based on position independent nucleon [2] or nuclear structure functions [3]. However, nuclear shadowing should depend on the parton's location inside the nucleus. If shadowing is due to gluon recombination [4], nuclear binding or rescaling [5], or other local phenomena, it should be proportional to the local nuclear density. The only studies of the spatial dependence have relied on qualitative impact parameter measurements, such as dark tracks in emulsion [6], to find evidence for such a spatial dependence.

This Rapid Communication presents calculations of the impact parameter dependence of nuclear shadowing on J/ψ and Drell-Yan production in heavy ion collisions. This spatial dependence has an important effect on the E_T dependence of J/ψ and Drell-Yan production if the quark and gluon distributions are shadowed differently. Since J/ψ suppression is a predicted signature of quark-gluon plasma formation [7], interpretations [2] of the anomalous suppression in the NA50 Pb+Pb data [1] should include the spatial dependence of the structure functions. We focus on shadowing alone, neglecting J/ψ absorption, to better illustrate the effect and present results for Pb+Pb collisions in the acceptance of the CERN NA50 experiment [1].

To be consistent with the NA50 analysis, we calculate J/ψ and Drell-Yan production to leading order (LO) where J/ψ production is dominated by gluon fusion while Drell-Yan production is due to $q\bar{q}$ annihilation. Then the cross section for nuclei A and B colliding at impact parameter b with center-of-mass energy $\sqrt{s_{NN}}$ and producing a particle V (J/ψ or γ^*) with mass m at scale Q is

$$\frac{d\sigma_{AB}^V}{dydm^2d^2bd^2r} = \sum_{i,j} \int dz dz' F_i^A(x_1, Q^2, \vec{r}, z) \times F_j^B(x_2, Q^2, \vec{b} - \vec{r}, z') \frac{d\hat{\sigma}_{ij}^V}{dydm^2}, \quad (1)$$

where $\hat{\sigma}_{ij}^V$ is the partonic $ij \rightarrow V$ cross section. The nuclear parton densities, F_i^A , are the product of momentum fraction, x , and Q^2 independent nuclear densities, ρ_A ; position and atomic mass, A , independent nucleon parton densities, f_i^N ; and a shadowing function, S^i :

$$F_i^A(x, Q^2, \vec{r}, z) = \rho_A(s) S^i(A, x, Q^2, \vec{r}, z) f_i^N(x, Q^2), \quad (2)$$

where $s = \sqrt{r^2 + z^2}$. In the absence of shadowing, $S^i(A, x, Q^2, \vec{r}, z) \equiv 1$. We employ Woods-Saxon nuclear density distributions, $\rho_A(s) = \rho_0(1 + \omega(s/R_A)^2)/(1 + e^{(s-R_A)/d})$, where R_A, d, ω and ρ_0 are fit to electron scattering data [8]

We use the color evaporation model of J/ψ production [9] so that

$$\begin{aligned} & f_i^N(x_1, Q^2) f_j^N(x_2, Q^2) \frac{d\hat{\sigma}_{ij}^{J/\psi}}{dydm^2} \\ &= F_{J/\psi} K_{\text{th}} \left\{ f_g^N(x_1, Q^2) f_g^N(x_2, Q^2) \frac{\sigma_{gg}(m^2)}{m^2} \right. \\ & \quad + \sum_{q=u,d,s} [f_q^N(x_1, Q^2) f_q^N(x_2, Q^2) \\ & \quad \left. + f_{\bar{q}}^N(x_1, Q^2) f_{\bar{q}}^N(x_2, Q^2)] \frac{\sigma_{q\bar{q}}(m^2)}{m^2} \right\}, \quad (3) \end{aligned}$$

where $m^2 = x_1 x_2 s_{NN}$. The LO partonic $c\bar{c}$ cross sections are defined in [10]. The fraction of $c\bar{c}$ pairs that become J/ψ 's, $F_{J/\psi}$, is fixed at next-to-leading order (NLO) [9] and K_{th} is

TABLE I. The Drell-Yan extrapolated and measured cross sections in pp , Pb+Pb, and S+U collisions and the $J/\psi \rightarrow \mu^+ \mu^-$ cross section in Pb+Pb collisions in the NA50 acceptance with the GRV LO and MRS A' parton densities at $\sqrt{s_{NN}} = 17.3$ GeV. We have not included $K_{\text{exp}} = 2.4$ for GRV LO and 1.7 for MRS A' .

	Drell-Yan ($2.9 < m < 4.5$ GeV)			Drell-Yan ($4.2 < m < 9$ GeV)			J/ψ
	σ_{pp} (pb)	σ_{PbPb} (pb)	σ_{SU} (pb)	σ_{pp} (pb)	σ_{PbPb} (pb)	σ_{SU} (pb)	σ_{PbPb} (nb)
GRV LO							
$S=1$	16.6	12.7	13.3	2.31	1.66	1.76	1.61
$S=S_1$	–	12.8	13.5	–	1.61	1.72	1.64
$S=S_2$	–	12.5	13.1	–	1.56	1.67	1.84
$S=S_3$	–	11.9	12.6	–	1.48	1.61	2.04
MRS A'							
$S=1$	18.8	18.3	19.0	2.15	2.17	2.29	1.53
$S=S_1$	–	18.6	19.4	–	2.10	2.26	1.58
$S=S_2$	–	18.1	18.9	–	2.03	2.19	1.74
$S=S_3$	–	17.2	18.1	–	1.93	2.10	1.85

the ratio of the NLO to LO J/ψ cross sections. We take the GRV LO [11,12] nucleon parton distributions with $m_c = 1.3$ GeV and $Q = m_c$ as well as the MRS A' densities [13] with $m_c = 1.2$ GeV and $Q = 2m_c$ where m_c and Q are chosen to agree with data [9].

The LO Drell-Yan cross section depends on isospin since $\sigma_{pp}^{\text{DY}} \neq \sigma_{pn}^{\text{DY}} \neq \sigma_{np}^{\text{DY}} \neq \sigma_{nn}^{\text{DY}}$

$$\begin{aligned}
 & f_i^N(x_1, Q^2) f_j^N(x_2, Q^2) \frac{d\hat{\sigma}_{ij}^{\text{DY}}}{dy dm^2} \\
 &= K_{\text{exp}} \frac{4\pi\alpha^2}{9m^2 s_{NN}} \\
 & \times \sum_{q=u,d,s} e_q^2 \left[\left\{ \frac{Z_A}{A} f_q^p(x_1, Q^2) + \frac{N_A}{A} f_q^n(x_1, Q^2) \right\} \right. \\
 & \times \left. \left\{ \frac{Z_B}{B} f_q^p(x_2, Q^2) + \frac{N_B}{B} f_q^n(x_2, Q^2) \right\} + q \leftrightarrow \bar{q} \right], \quad (4)
 \end{aligned}$$

where Z_A and N_A are the number of protons and neutrons in the nucleus and $Q = m$. We assume that $f_u^p = f_d^n, f_d^p = f_u^n$, etc. In Eqs. (3) and (4), $x_{1,2} = Qe^{\pm y}/\sqrt{s_{NN}}$. The factor K_{exp} accounts for the rate difference between the calculations and the data.

Three parametrizations of shadowing, based on nuclear deep-inelastic scattering [14], are used. The first, $S_1(A, x)$, treats quarks, antiquarks, and gluons equally without Q^2 evolution [15]. The other two evolve with Q^2 and conserve baryon number and total momentum. The second, $S_2^i(A, x, Q^2)$, modifies the valence quarks, sea quarks, and gluons separately for $2 < Q < 10$ GeV [16]. The most recent, $S_3^i(A, x, Q^2)$, evolves each parton distribution separately for $Q \geq 1.5$ GeV [17]. The S_3 initial gluon distribution shows important antishadowing in the region $0.1 < x < 0.3$ with sea quark shadowing in the same x range. In contrast, S_2 has less gluon antishadowing and essentially no sea quark effect.

Since we assume that shadowing is proportional to the local nuclear density, the spatial dependence is defined as

$$S_{\text{WS}}^i = S^i(A, x, Q^2, \vec{r}, z) = 1 + N_{\text{WS}} [S^i(A, x, Q^2) - 1] \frac{\rho_A(s)}{\rho_0}, \quad (5)$$

where N_{WS} is chosen so that $(1/A) \int d^3s \rho_A(s) S_{\text{WS}}^i = S^i$, similar to [18]. For lead, $N_{\text{WS}} = 1.32$. At large radii, $s \gg R_A$

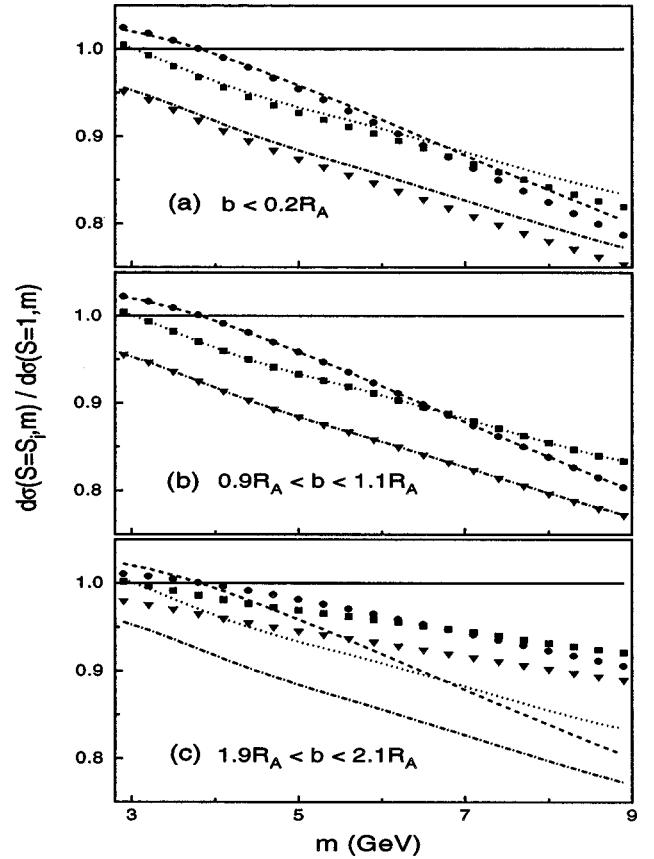


FIG. 1. The Drell-Yan dilepton mass spectrum, $d\sigma^{\text{DY}}/dm$, without and with spatial dependence relative to $S=1$ at $\sqrt{s_{NN}} = 17.3$ GeV. The curves correspond to b -averaged results with S_1 (dashed), S_2 (dotted), and S_3 (dot-dashed). The spatial dependence is illustrated for $S_{1,\text{WS}}$ (circles), $S_{2,\text{WS}}$ (squares), and $S_{3,\text{WS}}$ (triangles). The impact parameter ranges are (a) $0 < b < 0.2R_A$ fm, (b) $0.9R_A < b < 1.1R_A$ fm and (c) $1.9R_A < b < 2.1R_A$ fm respectively.

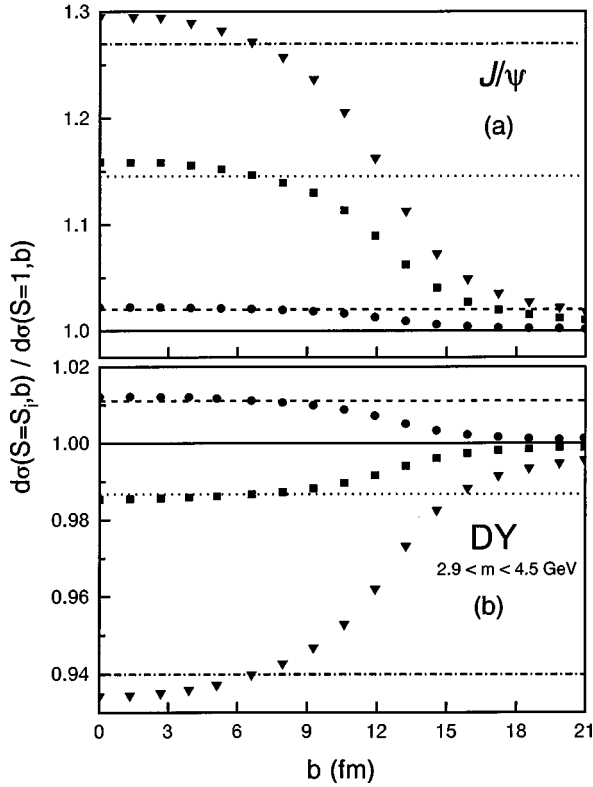


FIG. 2. The (a) J/ψ and (b) Drell-Yan rates in Pb+Pb collisions at $\sqrt{s_{NN}}=17.3$ GeV relative to production without shadowing, $S=1$, as a function of impact parameter. The curves and symbols are defined in Fig. 1.

and $S_{\text{WS}}^i \rightarrow 1$, while at the nuclear center, the modifications are larger than the average S^i . An alternative parametrization, S_{R}^i , proportional to the nuclear thickness [19,20], leads to a slightly larger modification in the nuclear core.

We adapt our calculations to the NA50 acceptance: center-of-mass rapidity $0 < y_{\text{c.m.}} < 1$ and Collins-Soper decay angle $|\cos \theta_{\text{CS}}| < 0.5$ [1]. The Drell-Yan spectrum is measured for $m > 4.2$ GeV and the factor K_{exp} is found by comparing LO calculations, Eq. (4), using the GRV LO distributions [12] with data. The ratio $\sigma^{J/\psi}/d\sigma^{\text{DY}}$, where $\sigma^{J/\psi}$ includes the branching ratio to $\mu^+\mu^-$, is formed by extrapolating the calculations to $2.9 < m < 4.5$ GeV with the same K_{exp} because J/ψ and ψ' decays dominate the region $2.7 < m < 3.5$ GeV. Table I gives the impact parameter averaged cross sections per nucleon pair for the GRV LO and MRS A' distributions for pp , Pb+Pb, and S+U interactions. We show the effects of isospin and shadowing at $\sqrt{s_{NN}}=17.3$ GeV. With the MRS A' set, the isospin correction is quite small in the extrapolated region [21]. Because isospin is unimportant in J/ψ production, only the Pb+Pb cross section is shown. However, the J/ψ results suggest that the AB dependence might be stronger if shadowing could be removed from the data. Although the choice of parton densities influences the isospin correction and K_{exp} , the average Drell-Yan shadowing is changed by less than 1% while the J/ψ shadowing changes as much as 5%, because the nuclear gluon distribution is imprecisely measured. The table shows that the dependence on the nuclear species is weak. The results also change by $\sim 1\%$ at $\sqrt{s_{NN}}=19.4$ GeV. Most impor-

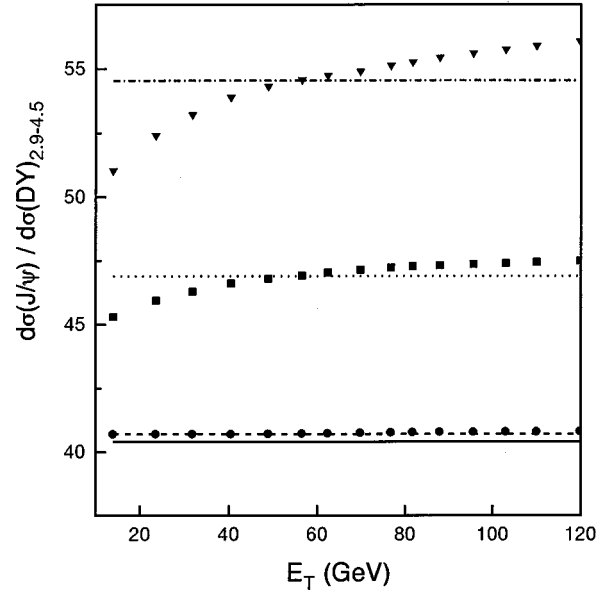


FIG. 3. The ratio of $J/\psi \rightarrow \mu^+\mu^-$ to Drell-Yan production, as a function of transverse energy, E_T , in the NA50 acceptance. The curves and symbols are defined in Fig. 1.

tant is the mass interval: shadowing is 5% stronger in the measured region than the extrapolated region.

To illustrate how shadowing could affect the interpretation of J/ψ suppression, Fig. 1 shows the Drell-Yan mass distribution relative to no shadowing, $S=1$. Shadowing changes the slope of the spectrum, producing an $\approx 20\%$ change in the predicted rate at $m \approx 9$ GeV. The similarity of valence and sea quark shadowing in S_1 causes this ratio to decrease faster with mass than S_2 or S_3 . Including only spatially averaged shadowing increases K_{exp} over that needed for $S=1$ in the measured relative to the extrapolated region, shown in Table I, as well as further increases the discrepancy in central collisions while overestimating K_{exp} in peripheral collisions. At small radii, Fig. 1(a), $d\sigma^{\text{DY}}/dm$ drops faster than the impact parameter averaged spectra. When $b \approx R_A$, Fig. 1(b), the averaged and spatial dependent spectra approximately coincide. At large radii, Fig. 1(c), shadowing is reduced, approaching $S=1$. These results show that using a calculation to extrapolate to an unmeasured region is problematic.

Figure 2 shows the impact parameter dependence of the J/ψ and Drell-Yan cross sections. The x_2 ranges nearly coincide: the Drell-Yan region $2.9 < m < 4.5$ GeV corresponds to $0.062 < x_2 < 0.26$ while the J/ψ range is $0.066 < x_2 < 0.18$. Since all three parametrizations assume some gluon anti-shadowing in this region, $\sigma^{J/\psi}$ is always enhanced.¹ Because S_1 is the same for quarks and gluons, J/ψ and Drell-Yan are equally affected by shadowing. On other hand, $S_{2,3}^q \leq 1$, reducing σ^{DY} .

In Fig. 3, $\sigma^{J/\psi}/\sigma^{\text{DY}}$, calculated in Eqs. (1)–(4), is pre-

¹We have compared our J/ψ calculations with nonrelativistic QCD calculations of quarkonium production [22] and found that the results are within 2–3% of those given here. Thus the shadowing ratios do not depend strongly on the J/ψ production model at this energy.

sented as a function of E_T . The correlation between E_T and b is based on the number of nucleon participants [2], in agreement with the most recent NA50 E_T distributions [21]. The Drell-Yan cross section is corrected for isospin to pp from Pb+Pb interactions with Eq. (4), following the NA50 analysis [1]. After the isospin adjustment, when $S=1$, $\sigma^{J/\psi}/\sigma^{\text{DY}} \sim 40.3$ at $\sqrt{s_{NN}}=17.3$ GeV and ~ 39.3 at 19.4 GeV, in reasonable agreement with the rescaled NA50 pp data [1]. The combined Drell-Yan shadowing and J/ψ anti-shadowing in Fig. 2 increases $\sigma^{J/\psi}/\sigma^{\text{DY}}$ to 40.6 with S_1 , 46.8 for S_2 and 54.4 using S_3 . The S_1 ratio is essentially independent of E_T since S_1 does not depend on the parton type or Q^2 and the x ranges of J/ψ and Drell-Yan production are very similar. However, S_2 and S_3 vary more with E_T . The S_2 ratio rises about 7% while the S_3 ratio increases $\approx 11\%$ as $\langle E_T \rangle$ grows from 14 GeV to 120 GeV. These enhancements are opposite to the observed drop at large E_T and small b [1].

Because of uncertainties in the gluon shadowing parametrization, it is difficult to draw detailed conclusions. However, S_1 should represent a lower limit and S_3 an upper limit. A stronger spatial dependence such as S_R^i [19] would slightly increase the effect with E_T while parametrizations based on, e.g. nuclear binding [5] might predict a smaller effect.

In conclusion, we have studied the impact parameter dependence of the ratio $\sigma^{J/\psi}/\sigma^{\text{DY}}$ using a spatially dependent

shadowing model. We find that the ratio increases at small b (large E_T) compared with more peripheral collisions. The magnitude of the effect depends on the shadowing parametrization. Neglecting shadowing could increase K_{exp} at $\sqrt{s_{NN}}=17.3$ GeV since the measured cross section is more strongly affected by shadowing than the extrapolated cross section. In addition, using an impact parameter averaged spectra in central collisions would tend to underestimate the total number of Drell-Yan pairs, increasing $\sigma^{J/\psi}/\sigma^{\text{DY}}$. If this effect could be identified and corrected for in the data, then $\sigma^{J/\psi}/\sigma^{\text{DY}}$ would rise $\sim 10\%$ at low E_T and drop $\sim 4\%$ at high E_T , enhancing the discrepancy between absorption models and the data. At higher $\sqrt{s_{NN}}$, such as at future heavy-ion colliders, the shadowing effect will be larger [23] since these colliders probe lower x values.

V.E. and A.K. would like to thank the LBNL RNC group for hospitality and M. Strikhanov and V.V. Grushin for discussions and support. R.V. would like to thank J. Schukraft for discussions. We also thank K.J. Eskola for providing the shadowing routines and for discussions. This work was supported in part by the Division of Nuclear Physics of the Office of High Energy and Nuclear Physics of the U. S. Department of Energy under Contract No. DE-AC03-76SF00098.

-
- [1] M.C. Abreu *et al.*, NA50 Collaboration, Phys. Lett. B **410**, 337 (1997); **410**, 327 (1997).
- [2] For a recent review, see R. Vogt, Phys. Rep. **310**, 197 (1999).
- [3] S. Gupta and H. Satz, Z. Phys. C **55**, 391 (1992); N. Hammon, L. Gerland, H. Stöcker, and W. Greiner, hep-ph/9807546.
- [4] L.V. Gribov, E.M. Levin, and M.G. Ryskin, Phys. Rep. **100**, 1 (1983).
- [5] S. Kumano and F.E. Close, Phys. Rev. C **41**, 1855 (1990).
- [6] T. Kitagaki *et al.*, Phys. Lett. B **214**, 281 (1988).
- [7] T. Matsui and H. Satz, Phys. Lett. B **178**, 416 (1986).
- [8] C.W. deJager, H. deVries, and C. deVries, At. Data Nucl. Data Tables **14**, 485 (1974).
- [9] R.V. Gavai, D. Kharzeev, H. Satz, G. Schuler, K. Sridhar, and R. Vogt, Int. J. Mod. Phys. A **10**, 3043 (1995); G.A. Schuler and R. Vogt, Phys. Lett. B **387**, 181 (1996).
- [10] B.L. Combridge, Nucl. Phys. **B151**, 429 (1979).
- [11] S. Gavin, S. Gupta, R. Kauffman, P. V. Ruuskanen, D. K. Srivastava, and R. L. Thews, Int. J. Mod. Phys. A **10**, 2961 (1995).
- [12] M. Glück, E. Reya, and A. Vogt, Z. Phys. C **53**, 127 (1992).
- [13] A.D. Martin, R.G. Roberts, and W.J. Stirling, Phys. Lett. B **354**, 155 (1995).
- [14] M. Arneodo, Phys. Rep. **240**, 301 (1994); M.R. Adams *et al.*, Phys. Rev. Lett. **68**, 3266 (1992).
- [15] K.J. Eskola, J. Qiu, and J. Czyzewski, private communication.
- [16] K.J. Eskola, Nucl. Phys. **B400**, 240 (1993).
- [17] K.J. Eskola, V.J. Kolhinen, and P.V. Ruuskanen, Nucl. Phys. **B535**, 351 (1998); K.J. Eskola, V.J. Kolhinen, and C.A. Salgado, hep-ph/9807297.
- [18] P. Castorina and A. Donnachie, Z. Phys. C **49**, 481 (1991).
- [19] V. Emel'yanov, A. Khodinov, S.R. Klein, and R. Vogt, Phys. Rev. C **56**, 2726 (1997).
- [20] V. Emel'yanov, A. Khodinov, S.R. Klein, and R. Vogt, Phys. Rev. Lett. **81**, 1801 (1998); K.J. Eskola, Z. Phys. C **51**, 633 (1991).
- [21] A. Romana *et al.*, NA50 Collaboration, in Proceedings of the 33rd Rencontres de Moriond, QCD and High Energy Hadronic Interactions, Les Arcs, France, 1998.
- [22] G.T. Bodwin, E. Braaten, and G.P. Lepage, Phys. Rev. D **51**, 1125 (1995); M. Beneke and I.Z. Rothstein, *ibid.* **54**, 2005 (1996).
- [23] V. Emel'yanov, A. Khodinov, S.R. Klein, and R. Vogt, in preparation.